Supplementary Data

The influence of cross-linking density on the efficiency of post-synthetic sulfonation of hyper-cross-linked polymers and their adsorption capacity for antibiotic pollutants

Joanna Wolska[a,*], Malwina Muńko[b], Hussein EL Siblani[c], Igor Telegeiev[c], Marcin Frankowski[a], Anna Szwajca[a], Justyna Walkowiak-Kulikowska[a], Mohamad El-Roz[c], Lukasz Wolski[a]

[a] *Faculty of Chemistry, Adam Mickiewicz University, Poznań, ul. Uniwersytetu Poznańskiego 8, 61-614 Poznań, Poland*

[b] *Center for Advanced Technology, Adam Mickiewicz University, ul. Uniwersytetu Poznańskiego 10, 61-614 Poznań, Poland*

[c] *Laboratoire Catalyse et Spectrochimie, Normandie Université, ENSICAEN, UNICAEN, CNRS, Caen, 14050, France*

* *Corresponding author: j.wolska@amu.edu.pl (J. Wolska)*

Table of content:

Extended experimental section

Adsorption kinetic parameters were determined by using linearized form of the pseudo-first order (PFO) (Eq. S1) and pseudo-second order (PSO) (Eq. S2) models described by Ho and McKay [*Process Biochem.* 34 (1999) 451, doi:10.1016/S0032-9592(98)00112-5], where $q(t)$ and q_e are the amount of adsorbate adsorbed at any given time, t and at equilibrium, respectively, k_1 and k_2 corresponds to adsorption rate constant for pseudo-first order and pseudo-second order model, respectively.

$$\ln\left(q_e - q(t)\right) = -k_1 t + lnq_e \qquad \text{(Eq. S1)}$$

$$\frac{t}{t(q)} = \left(\frac{1}{q_e}\right) t + \frac{1}{k_2 q_e^2} \qquad \text{(Eq. S2)}$$

k_1 and k_2 values were determined by plotting $\ln\left(q_e - q(t)\right)$ vs t and $\frac{t}{t(q)}$ vs t for PFO and PSO, respectively. The kinetics parameters were then estimated from the slope and intercept of the best fit line such that, if m = slope and b = intercept, $k_1 = -m$ and $q_e = exp\ (b)$ for PFO, while $k_2 = \frac{m^2}{b}$ and $q_e = m^{-1}$ for PSO [*Clean. Eng. Technol.* 1 (2020) 100032, doi:10.1016/j.clet.2020.100032].

Experimental q_e value were estimated on the basis of adsorption tests using the following formula (Eq. S3):

$$q_e = \frac{V(C_0 - C_t)}{m} \qquad \text{(Eq. S3)}$$

where, C_0 is an initial concentration of antibiotic (mg/L), C_t is concentration of antibiotic (mg/L) after a given adsorption time, t (min), V is the volume of the reaction mixture (L), and m is the mass of the adsorbent (g).

Adsorption kinetics was also analyzed using Weber–Morris intraparticle diffusion (ID) model (Eq. S4) [*J. Sanit. Eng. Div. Am. Soc. Civ. Eng.* 89 (1963) 31, doi:10.1061/JSEDAI.0000430].

$$q_t = K_{id} t^{\frac{1}{2}} + C \qquad \text{(Eq. S4)}$$

where q_t is the adsorption capacity at any time (mg/g), K_{id} is the intraparticle diffusion rate constant (mg g^{-1} $min^{-1/2}$), t is the time taken for the adsorption process (min) and C is a constant for the any experiment (mg/g) that gives an idea about the thickness of the boundary layer. When a graph of q_t is plotted against $t^{\frac{1}{2}}$, a linear graph is obtained with regression linear coefficient, R^2, close to unity. The slope of the graph reveals the intraparticle diffusion rate constant, K_{id}, while intercept of the graph stands for C.

Adsorption isotherm parameters were determined by using linearized form of the Langmuir (Eq. S5) and Freundlich (Eq. S6) [*SN Appl. Sci.* 2 (2020) 187, doi:10.1007/s42452-020-1978-y].

$$\frac{C_e}{q_e} = \frac{1}{q_m}(C_e) + \frac{1}{q_m K_L} \qquad \text{(Eq. S5)}$$

$$\log_{10} q_e = \frac{1}{n}\log_{10} C_e + \log_{10} K_F \qquad \text{(Eq. S6)}$$

In the case of linear form of Langmuir model (Eq. S5), q_e is the amount of adsorbate per unit mass of adsorbent at equilibrium (mg/g), K_L is the adsorption capacity constant (L/g), C_e is the concentration of adsorbate at equilibrium (mg/L) and q_m is the maximum adsorption capacity (mg/g). When graph of $\frac{C_e}{q_e}$ is plotted against C_e, a linear graph is a acquired with regression linear coefficient, R^2, close to unity. The q_m and K_L are obtained from the slope and intercept of the graph. Both the slope and intercept of the graph represent the values for $\frac{1}{q_m}$ and $\frac{1}{q_m K_L}$, respectively.

In the case of linear form of Freundlich model (Eq. S6), where q_e is the amount of adsorbate per unit mass of adsorbent at equilibrium (mg/g), K_F is the adsorption capacity constant (L/g), C_e is the concentration of the adsorbate at equilibrium (mg/L), n is the heterogeneity factor and $\frac{1}{n}$ is the adsorption intensity. When a graph of $\log_{10} q_e$is plotted against $\log_{10} C_e$, a linear graph

is acquired with regression linear coefficient, R^2, close to unity. The n and K_F are obtained from the slope and intercept of the graph. Both the slope and intercept of the graph represent the values for $\frac{1}{n}$ and $\log_{10} K_F$, respectively.

Activation energy (E_a) was calculated using the linear form of Arrhenius equation (Eq. S7):

$$\ln k = -\frac{E_a}{RT} + \ln A \qquad \text{(Eq. S7)}$$

where, E_a (J mol^{-1}) is the apparent activation energy of the reaction; R is the ideal gas constant (8.314 J mol^{-1} K^{-1}), T is reaction temperature (K), k is a coefficient. Since the adsorption process is in accordance with pseudo-second order kinetic model, the apparent activation energy was calculated by the coefficient of k derived from pseudo-second order kinetic model. When a graph of $\ln k$ is plotted against $1/T$, a linear graph is acquired with regression linear coefficient, R^2, close to unity. The E_a is obtained from the slope of the graph. The slope of the graph represent the values for $-E_a/R$.

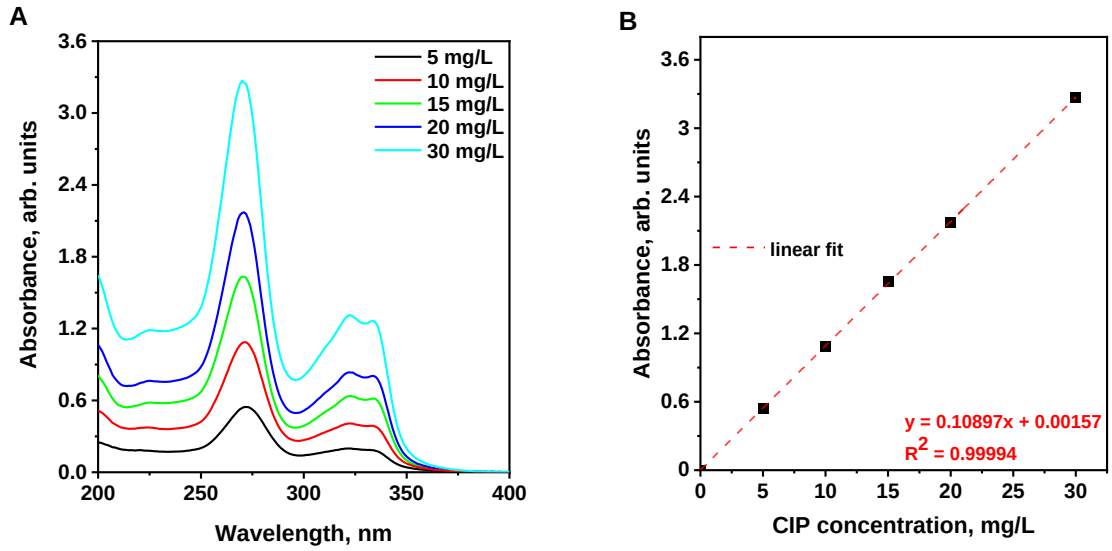

Fig. S1. (A) UV-vis spectra of CIP solution of different concentration. (B) Relationship between concentration of the CIP and its absorbance at λ_{max} = 271 nm.

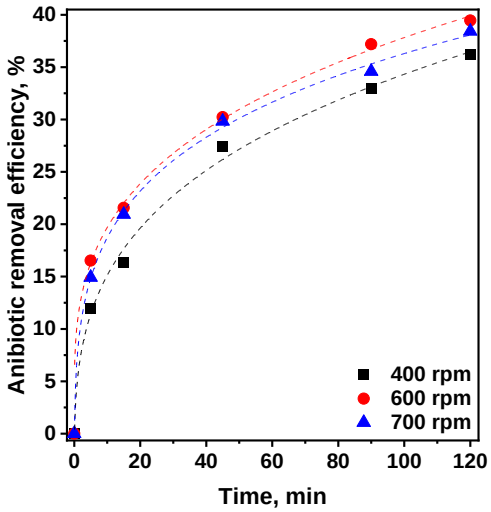

Fig. S2. The influence of stirring rate on the efficiency of CIP removal in the presence of HCP1. *Adsorption conditions*: 200 mL of ciprofloxacin solution (C_0 = 7.5 mg/L), 5 mg of the polymer (adsorbent loading = 0.025 g/L), initial pH ~ 6.5 (before addition of adsorbent), room temperature.

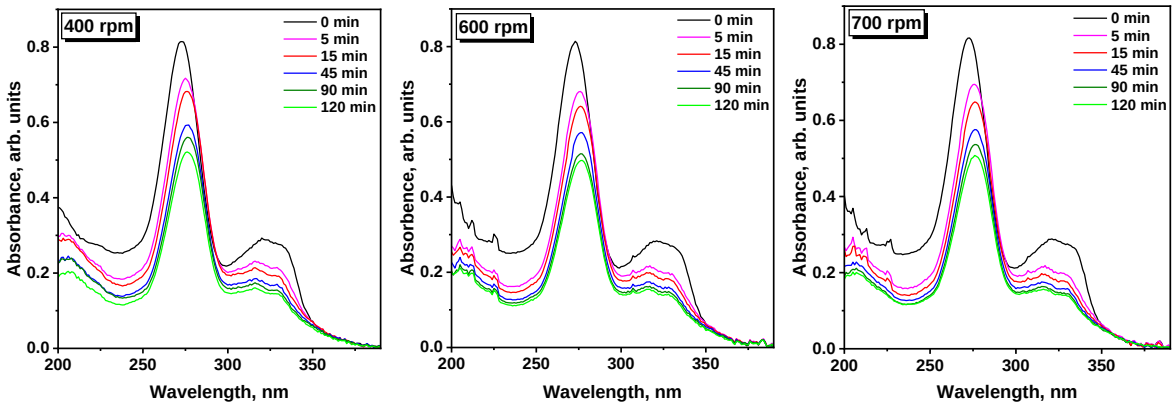

Fig. S3. UV-vis absorption spectra of liquid phase recorded during adsorptive removal of ciprofloxacin at different stirring rate in the presence of HCP1. *Adsorption conditions*: 200 mL of ciprofloxacin solution (C_0 = 7.5 mg/L), 5 mg of the polymer (adsorbent loading = 0.025 g/L), initial pH ~ 6.5 (before addition of the adsorbent), room temperature.

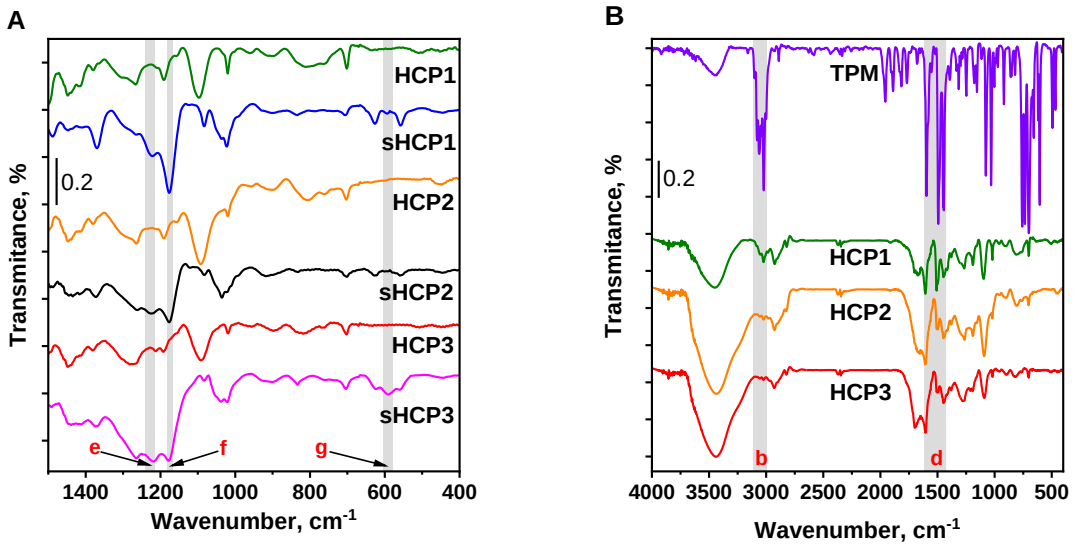

Fig. S4. (A) The fingerprint region of FTIR spectra of pristine and sulfonated HCPs (regions e and f: asymmetric and symmetric stretching vibrations of S=O bonds in $-SO_3H$ groups, respectively; region g: stretching vibration of C−S bond). (B) Comparative analysis of FTIR spectra of triphenylmethane monomer (TPM), HCP1, HCP2, and HCP3 polymers (region b: band in the region between 3100 and 3000 cm^{-1} assigned to the sp^2-hybridized C−H bonds of TPM core; region d: band in the region between 1600 and 1450 cm^{-1} assigned to the C=C bonds of TPM core).

Table S1. Sulfur content and acid exchange capacity of all investigated polymers.

Adsorbent	Sulfur content [wt%][a]	Sulfur content[a] [mmol/g]	Ion exchange capacity[b] [mmol/g]
sHCP1	7.13 ± 0.04	2.22 ± 0.03	2.71 ± 0.13
sHCP2	4.74 ± 0.01	1.48 ± 0.02	1.59 ± 0.07
sHCP3	3.82 ± 0.02	1.19 ± 0.02	1.46 ± 0.06
HCP1	n/a	n/a	0.19
HCP2	n/a	n/a	0.19
HCP3	n/a	n/a	0.19
Amberlyst-15	14.92 ± 0.03	4.66 ± 0.07	4.65 ± 0.23

[a] Average values derived from three measurements determined based on EA;

[b] Average values derived from three measurements determined based on acid-base titration method.

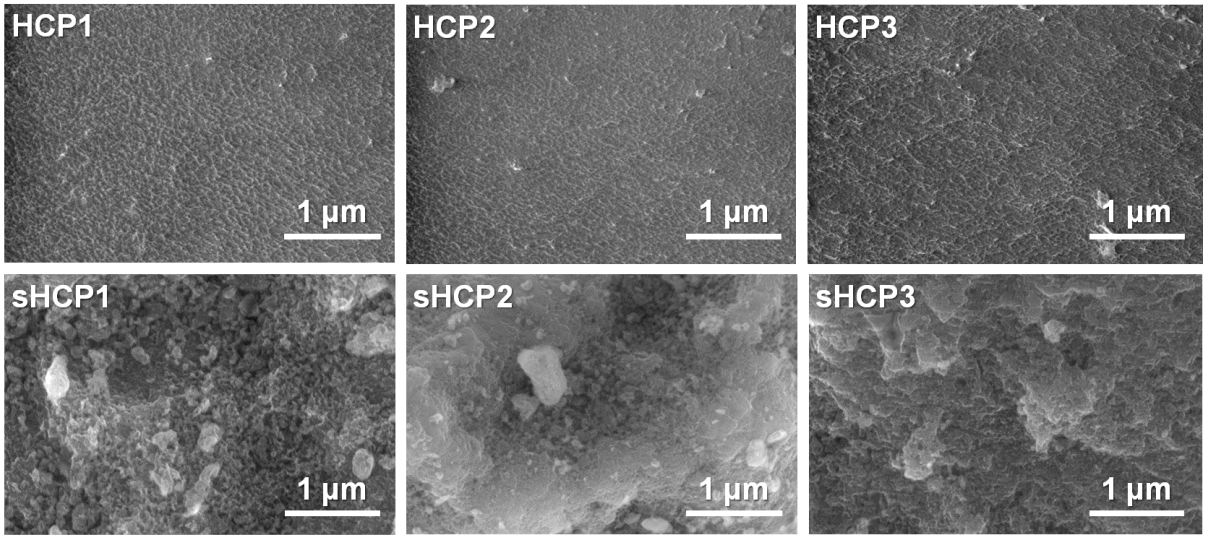

Fig. S5. SEM images of the pristine HCPs (top panel), and their sulfonated counterparts (bottom panel).

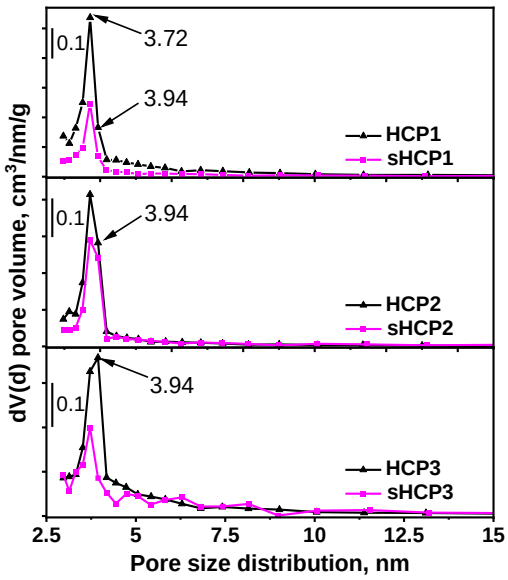

Fig. S6. Pore size distributions estimated for the investigated adsorbents from the desorption branch of the isotherms using the Barrett-Joyner-Halenda (BJH) method.

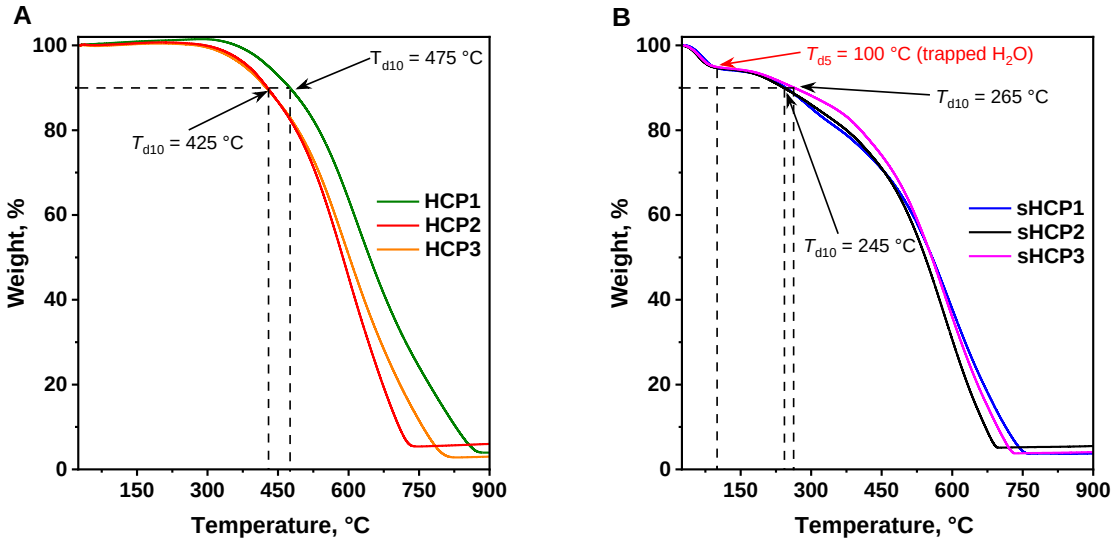

Fig. S7. Thermogravimetric profiles of (A) pristine HCPs, and (B) sulfonated HCPs. The red arrow indicates the 5% weight loss (T_{d5}) under nitrogen atmosphere. The black arrows indicate the decomposition temperatures of polymers at 10% weight loss (T_{d10}) under nitrogen atmosphere.

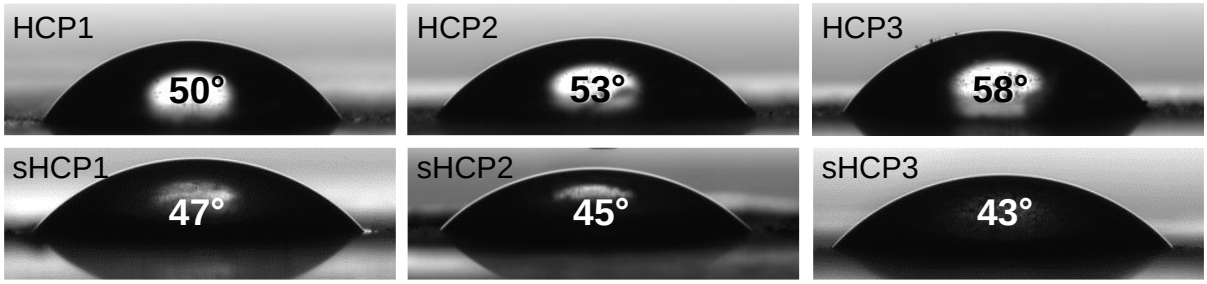

Fig. S8. The water contact angle (CA) of pristine HCPs (top panel), and their sulfonated counterparts (bottom panel) obtained with the sessile drop technique.

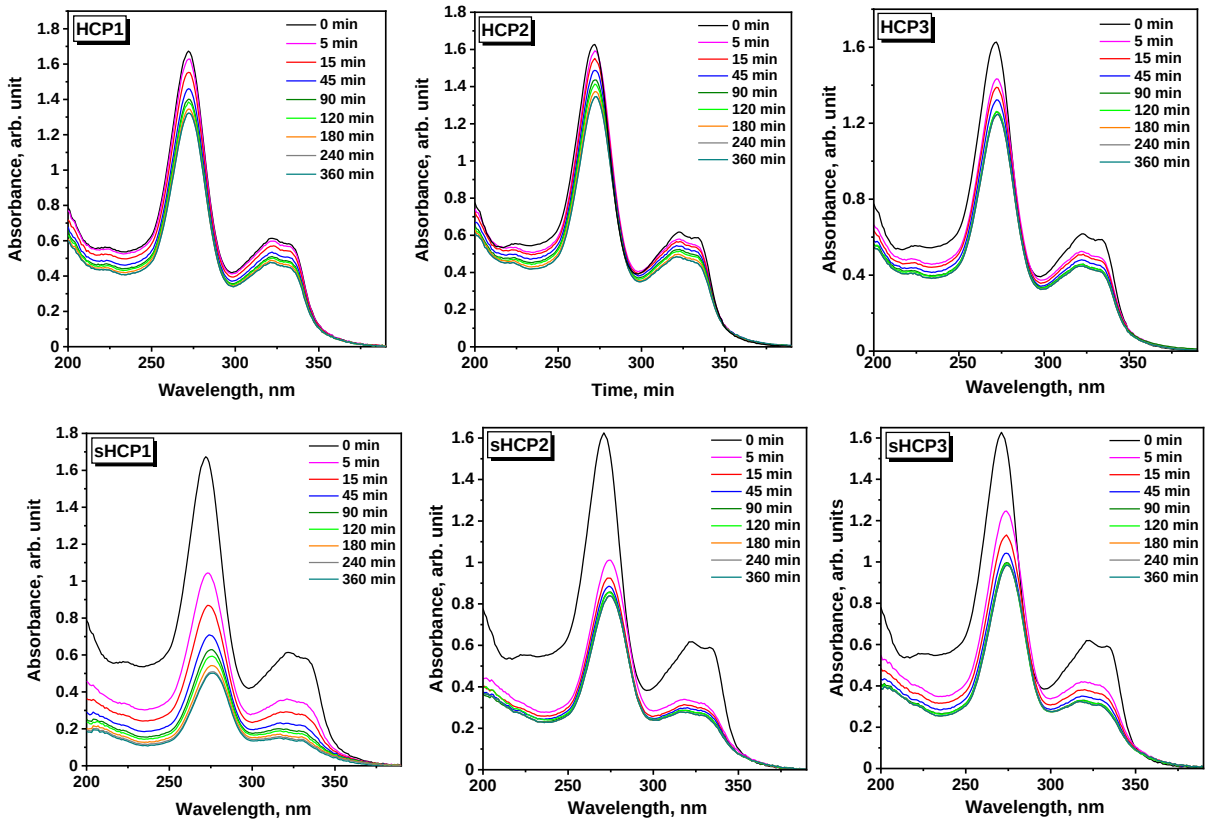

Fig. S9. UV-vis absorption spectra of liquid phase recorded during adsorptive removal of CIP in the presence of HCP1, HCP2, HCP3 and their sulfonated counterparts sHCP1, sHCP2 and sHCP3. *Adsorption conditions*: 200 mL of CIP solution (C_0 = 15 mg/L), 5 mg of polymer (adsorbent loading = 0.025 g/L), initial pH ~ 6.5 (before addition of the adsorbent), room temperature, stirring rate: 600 rpm.

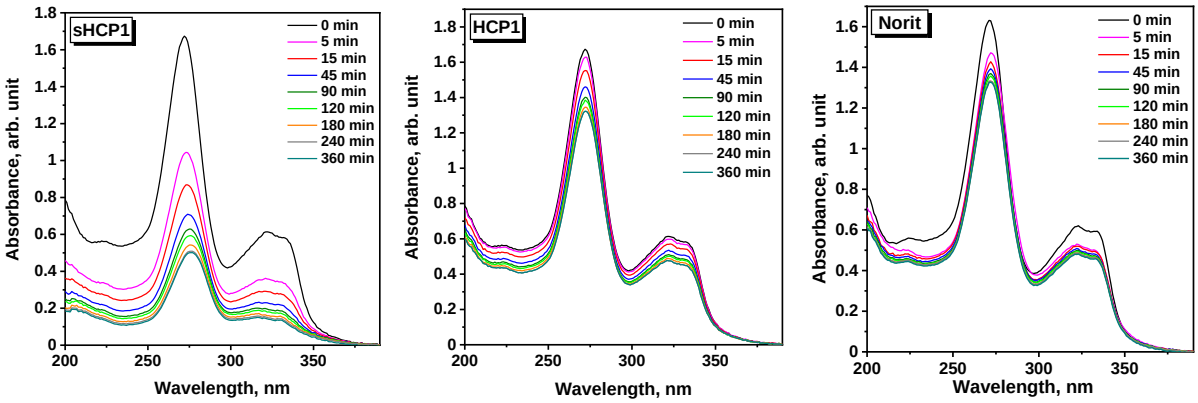

Fig. S10. UV-vis absorption spectra of liquid phase recorded during adsorptive removal of CIP in the presence of sHCP1, HCP1 and commercial *Norit*. *Adsorption conditions*: 200 mL of CIP solution (C_0 = 15 mg/L), 5 mg of adsorbent (adsorbent loading = 0.025 g/L), initial pH ~ 6.5 (before addition of the adsorbent), room temperature, stirring rate: 600 rpm.

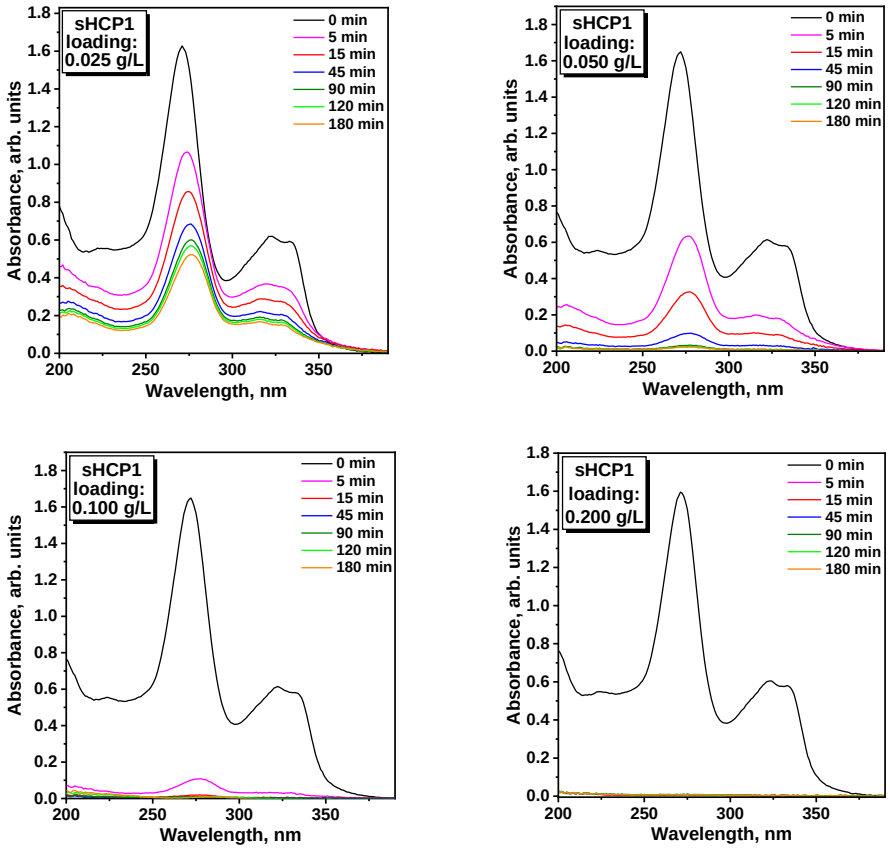

Fig. S11. UV-vis absorption spectra of liquid phase recorded during adsorptive removal of CIP at different sHCP1 loadings. *Adsorption conditions*: 200 mL of ciprofloxacin solution (C_0 = 15 mg/L), initial pH ~ 6.5 (before addition of the adsorbent), room temperature, stirring rate: 600 rpm.

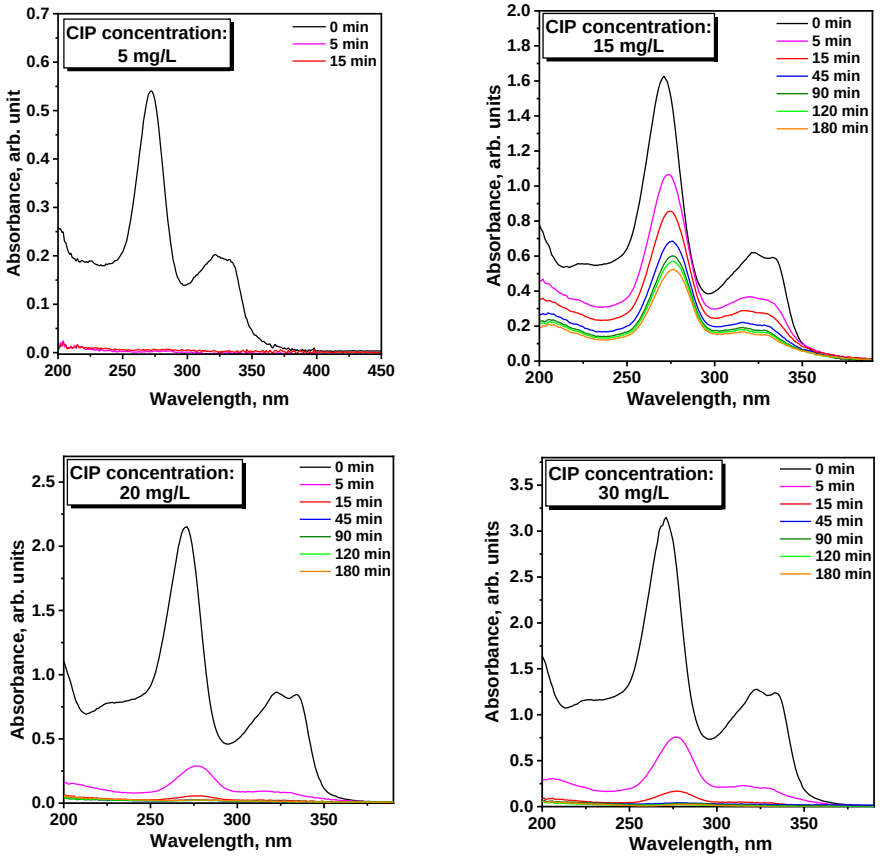

Fig. S12. UV-vis absorption spectra of liquid phase recorded during adsorptive removal of CIP studied at different initial concentration of the antibiotic in the presence of sHCP1. *Adsorption conditions*: 200 mL of CIP solution, 20 mg of the polymer (adsorbent loading = 0.100 g/L), initial pH ~ 6.5 (before addition of the adsorbent), room temperature, stirring rate: 600 rpm.

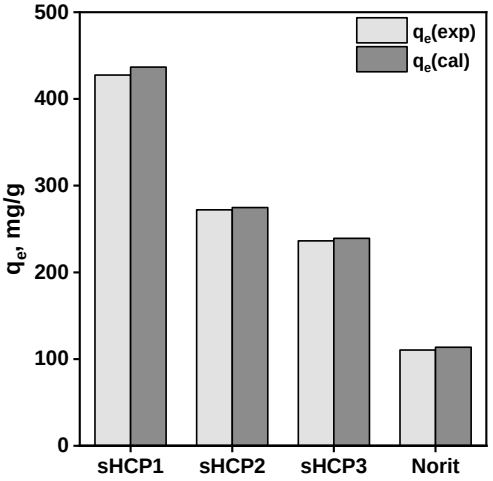

Fig. S13. Comparison of maximum adsorption capacity of CIP on sHCP1, sHCP2, sHCP3 and commercial *Norit* adsorbents derived from the experiments (q_e(exp)), and calculated from the PSO kinetic model (q_e(cal)).

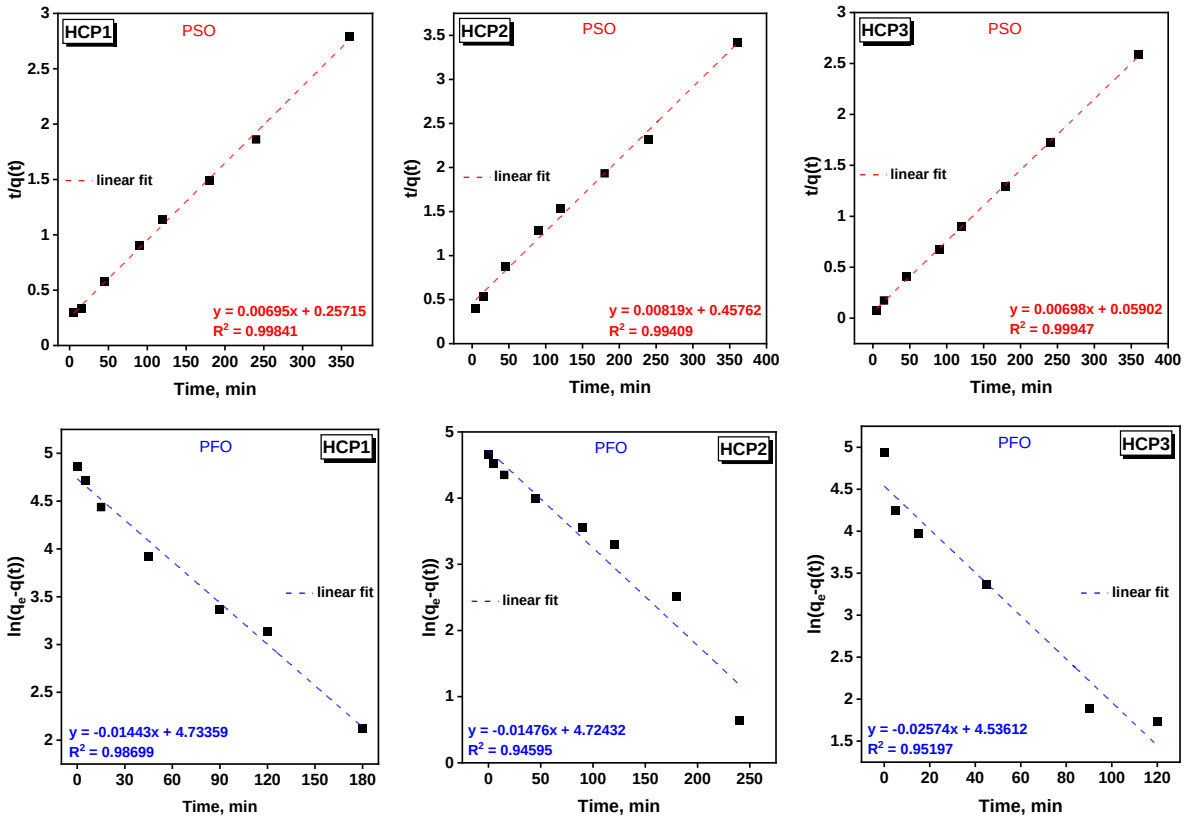

Fig. S14. Graphs used for assessing the CIP adsorption kinetics on the HCP1, HCP2 and HCP3 adsorbents. PFO and PSO stand for pseudo-first order and pseudo-second order kinetic model, respectively. *Adsorption conditions:* 200 mL of the antibiotic solution (C_0 = 15 mg/L), 5 mg of sHCP1 (adsorbent loading = 0.025 g/L), initial pH ~ 6.5 (before addition of the adsorbent), room temperature, stirring rate: 600 rpm.

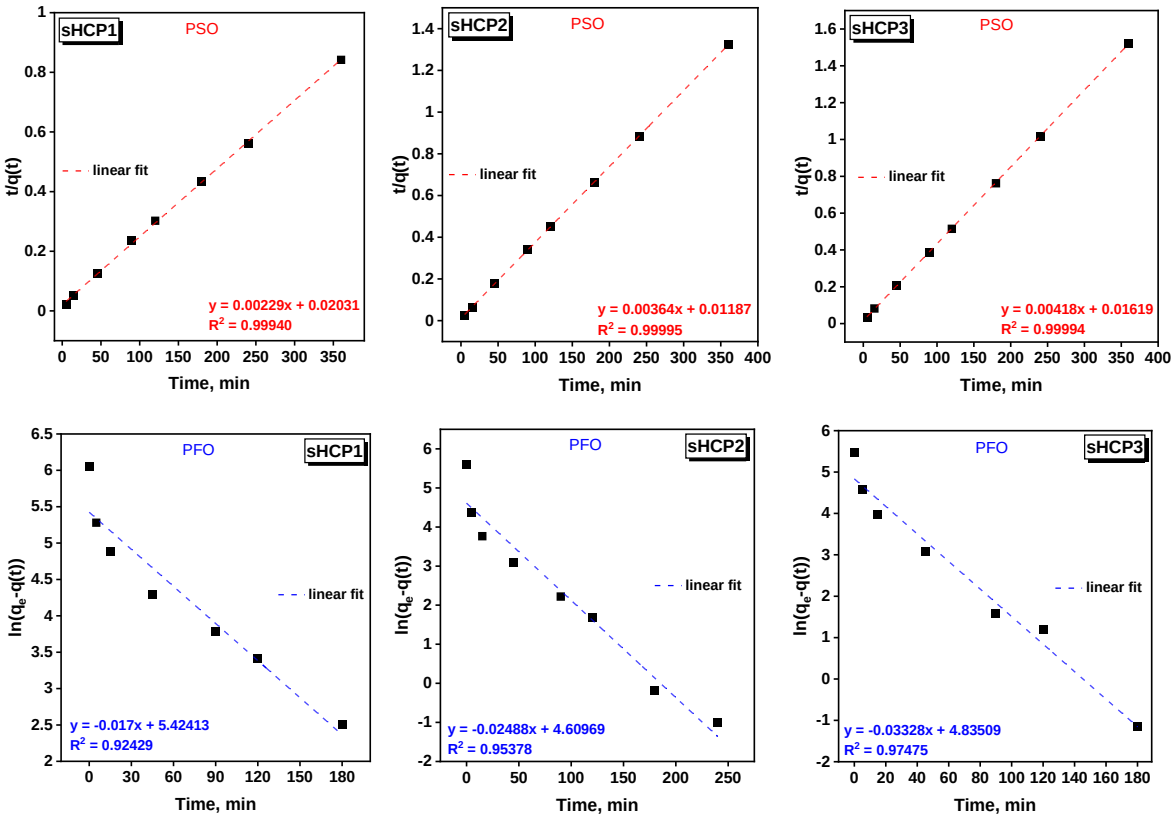

Fig. S15. Graphs used for assessing the CIP adsorption kinetics on the sHCP1, sHCP2 and sHCP3 adsorbents. PFO and PSO stand for pseudo-first order and pseudo-second order kinetic model, respectively. *Adsorption conditions:* 200 mL of the antibiotic solution (C_0 = 15 mg/L), 5 mg of sHCP1 (adsorbent loading = 0.025 g/L), initial pH ~ 6.5 (before addition of the adsorbent), room temperature, stirring rate: 600 rpm.

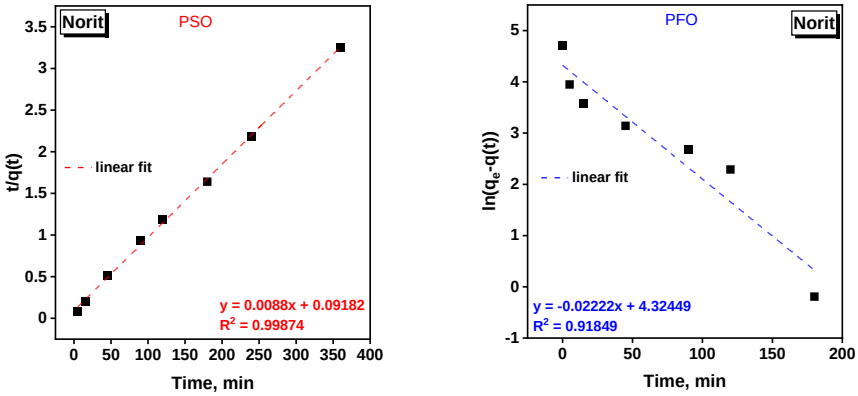

Fig. S16. Graphs used for assessing the CIP adsorption kinetics on the commercial *Norit* adsorbent. PFO and PSO stand for pseudo-first order and pseudo-second order kinetic model, respectively. *Adsorption conditions:* 200 mL of the antibiotic solution (C_0 = 15 mg/L), 5 mg of sHCP1 (adsorbent loading = 0.025 g/L), initial pH ~ 6.5 (before addition of the adsorbent), room temperature, stirring rate: 600 rpm.

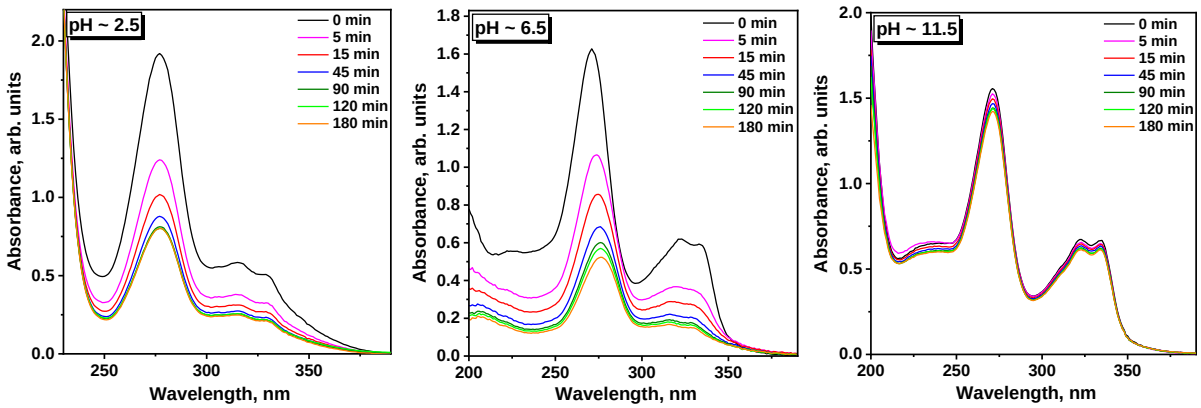

Fig. S17. UV-vis absorption spectra of liquid phase recorded during adsorptive removal of CIP in the presence of sHCP1 at different initial pH values. *Adsorption conditions*: 200 mL of the antibiotic solution (C_0 = 15 mg/L), 5 mg of the polymer (adsorbent loading = 0.025 g/L), room temperature, stirring rate: 600 rpm.

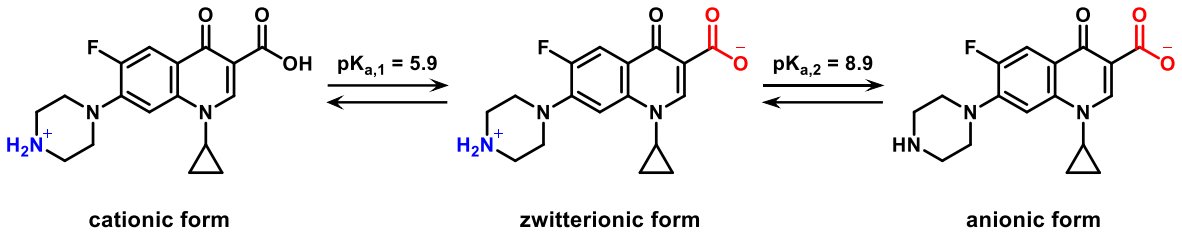

Fig. S18. Speciation of CIP at different pH values [*J. Ind. Eng. Chem.* 93 (2021) 57, doi: 10.1016/j.jiec.2020.09.023].

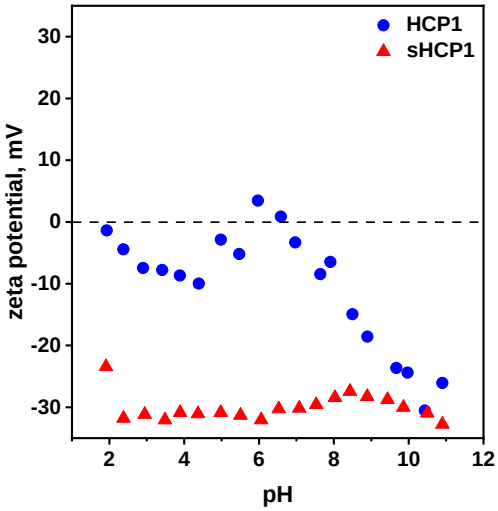

Fig. S19. Surface zeta potential of HCP1 and sHCP1 displayed as a function of pH.

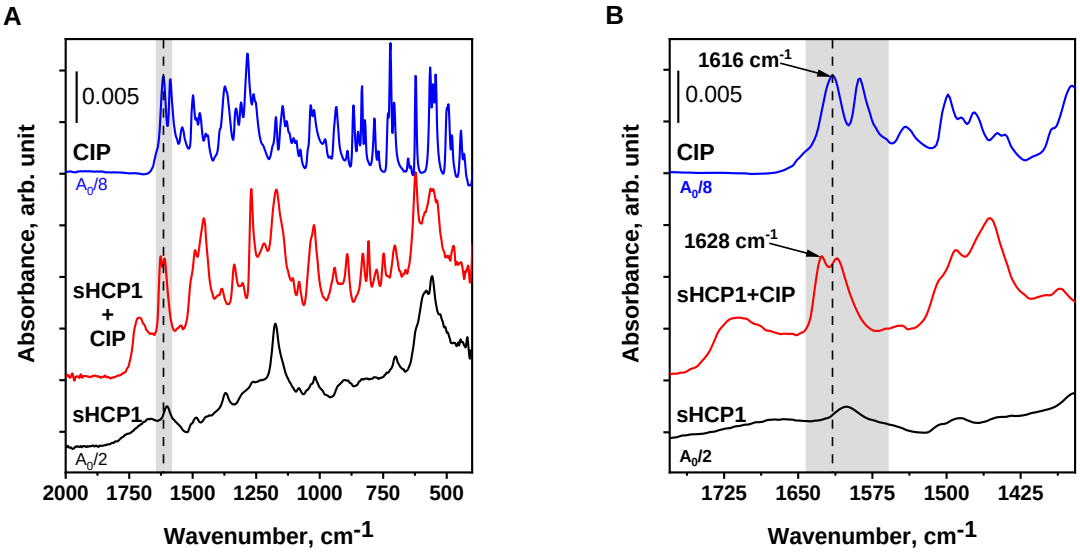

Fig. S20. Comparative analysis of FTIR-ATR spectra of spent sHCP1 after CIP adsorption (sHCP1+CIP) with powdered CIP and fresh sHCP1 in the range of the (A) 2000-400 cm^{-1}, and (B) 1780-1370 cm^{-1}. The range highlighted in gray corresponds to the band attributed to N-H bending vibrations in the amino group in the piperazine moiety of CIP.

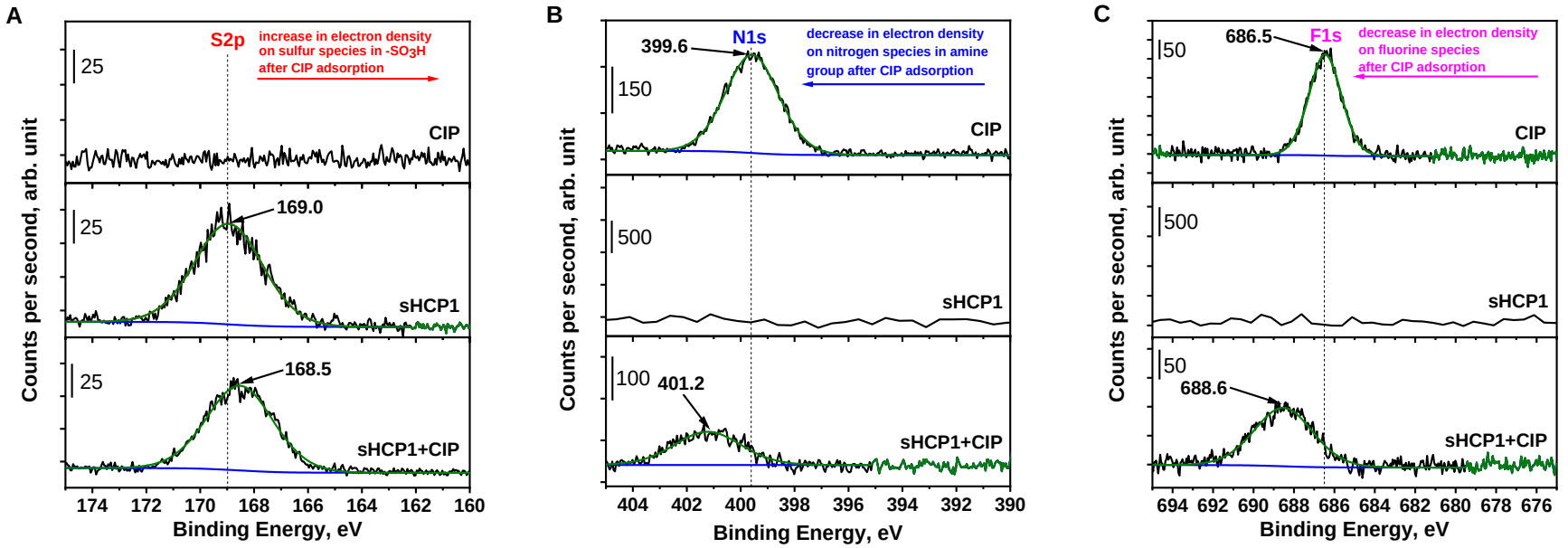

Fig. S21. Comparison of XPS spectra of sHCP1 after CIP adsorption (sHCP1+CIP), powdered CIP and fresh sHCP1 in the (A) S2p (B) N1s, and (C) F1s energy range.

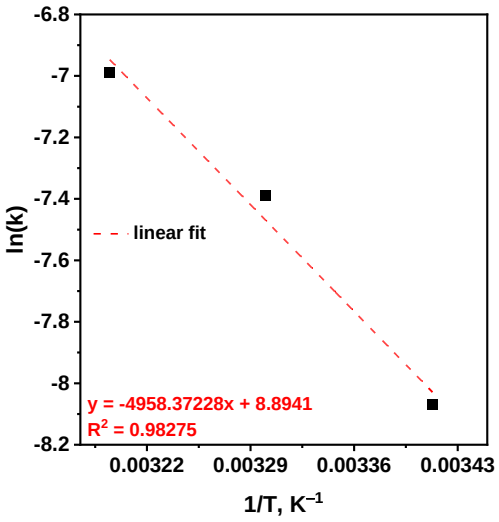

Fig. S22. Arrhenius plot for ciprofloxacin adsorption on sHCP1.

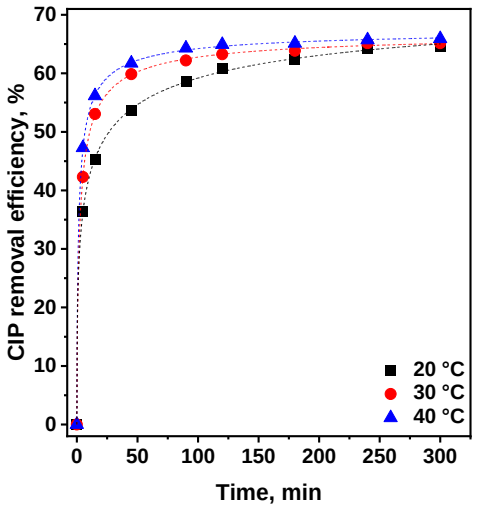

Fig. S23. The effect of temperature on ciprofloxacin removal in the presence of sHCP1. *Adsorption conditions*: 100 mL of CIP solution (C_0 = 30 mg/L), 5 mg of the polymer (adsorbent loading = 0.025 g/L), initial pH ~ 6.5 (before addition of the adsorbent), stirring rate: 600 rpm. Experiments performed using Easy-Max (Mettler-Toledo) work station.

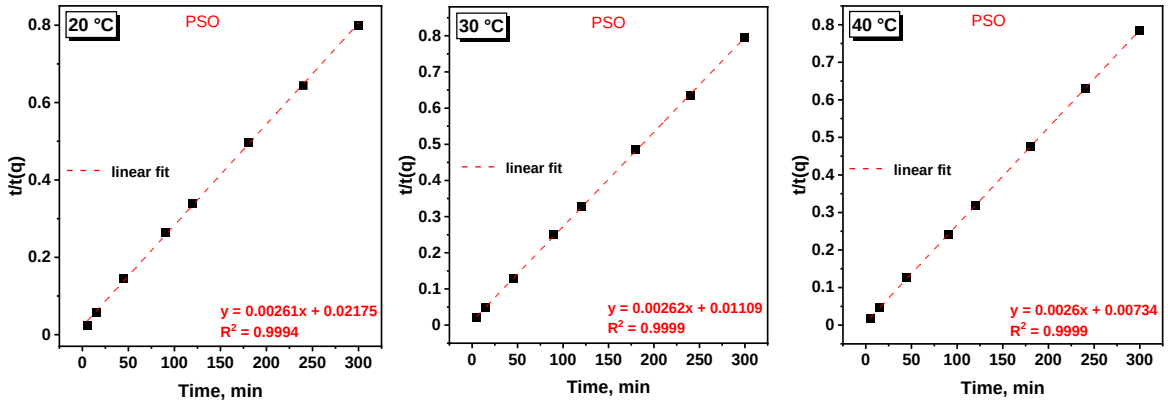

Fig. S24. Graphs used for assessing the pseudo-second order (PSO) kinetic model for the CIP adsorption on the sHCP1 adsorbent at different temperature. *Adsorption conditions:* 100 mL of the antibiotic solution (C_0 = 30 mg/L), 5 mg of sHCP1 (adsorbent loading = 0.025 g/L), initial pH ~ 6.5 (before addition of the adsorbent), stirring rate: 600 rpm. Experiments performed using Easy-Max (Mettler-Toledo) work station.

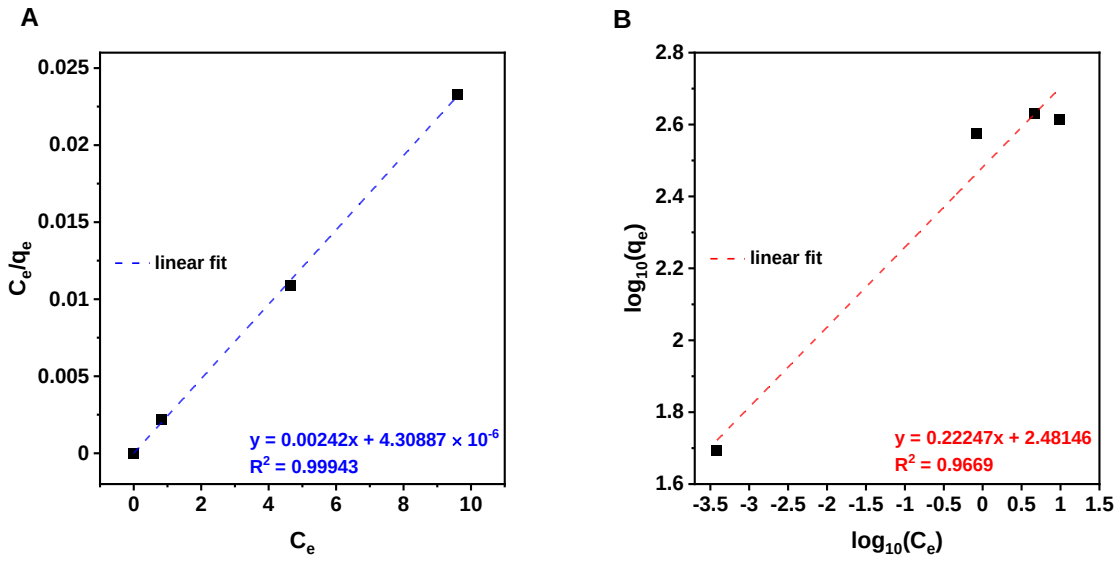

Fig. S25. (A) Langmuir and (B) Freundlich adsorption isotherm models for the adsorption of ciprofloxacin on sHCP1 adsorbent. *Adsorption conditions*: 200 mL of CIP solution (C_0 = 5.0 10.0, 15.0 or 20.0 mg/L), 5 mg of the polymer (adsorbent loading = 0.025 g/L), initial pH ~ 6.5 (before addition of the adsorbent), room temperature, stirring rate: 600 rpm.

Table S2. Adsorption parameters derived from Langmuir and Freundlich adsorption isotherm models.

Freundlich				Langmuir		
K_F [L/g]	n	$1/n$	R^2	K_L [L/g]	q_m [mg/g]	R^2
303.01	4.49	0.22	0.9669	561.63	413.22	0.9994

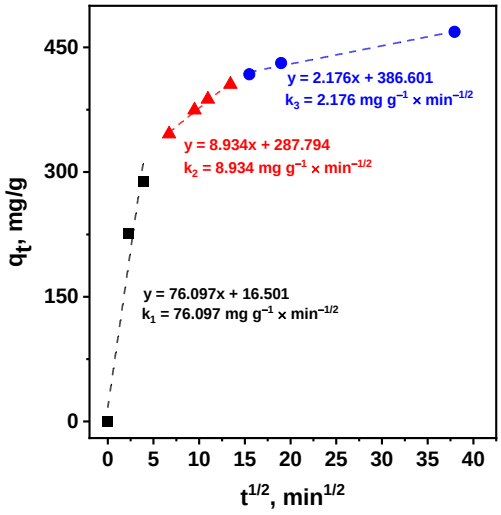

Fig. S26. The Weber-Morris intraparticle diffusion (ID) model for the adsorption of ciprofloxacin on sHCP1 adsorbent.

Table S3. Main characteristics of four studied antibiotics.

Parameter	Ciprofloxacin	Tetracycline	Amoxicillin	Sulfamethoxazole
Chemical structure	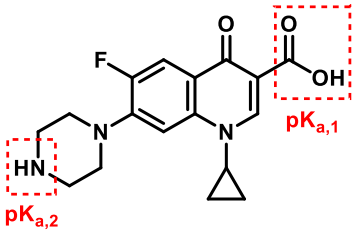	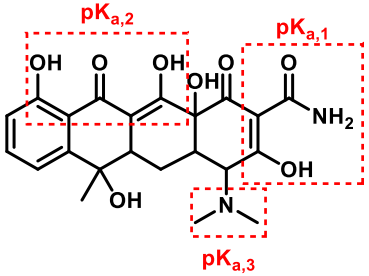	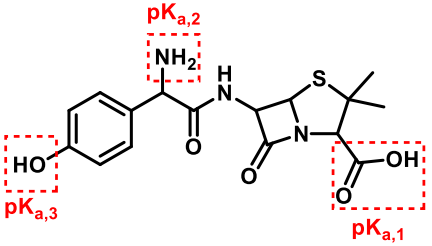	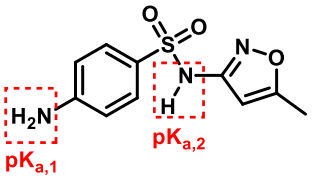
Antibiotic class	quinolones	tetracyclines	β-lactams	sulfonamides
Abbreviation	CIP	TC	AMX	SMX
Chemical formula	$C_{17}H_{18}FN_3O_3$	$C_{22}H_{24}N_2O_8$	$C_{16}H_{19}N_3O_5S$	$C_{10}H_{11}N_3O_3S$
Molecular weight [g/mol]	331.35	444.44	365.40	253.28
pKa	5.9 ($pK_{a,1}$); 8.9 ($pK_{a,2}$)	3.3 ($pK_{a,1}$); 7.8 ($pK_{a,2}$); 9.6 ($pK_{a,3}$)	2.7 ($pK_{a,1}$); 7.5 ($pK_{a,2}$); 9.6 ($pK_{a,3}$)	1.8 ($pK_{a,1}$); 5.6 ($pK_{a,2}$)
Reference	*J. Ind. Eng. Chem.* 93 (2021) 57, doi:10.1016/j.jiec.2020.09.023	*Chromatogr. Res. Int.* 2012 (2012) 1, doi:10.1155/2012/135854	*Sci. Total Environ.* 408 (2010) 6272, doi:10.1016/j.scitotenv.2010.08.058	*Water Res.* 38 (2004) 2874, doi: 10.1016/j.watres.2004.03.017.

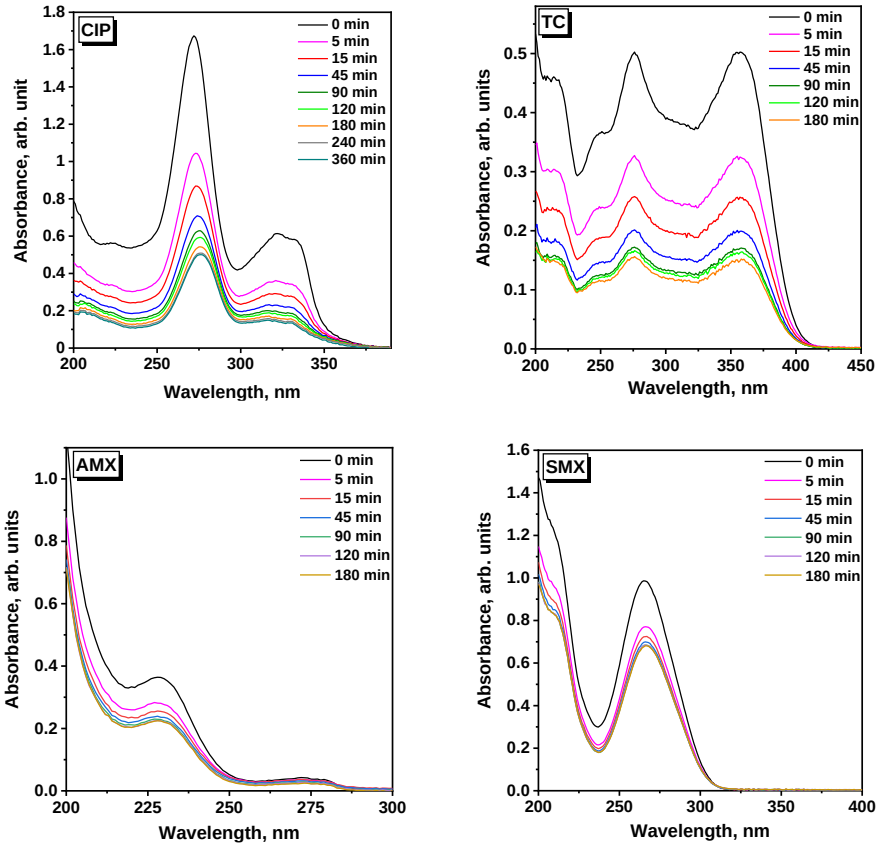

Fig. S27. UV-vis absorption spectra of liquid phase recorded during adsorptive removal of studied antibiotics in the presence of sHCP1. *Adsorption conditions*: 200 mL of the antibiotic solution (C_0 = 15 mg/L), 5 mg of the polymer (adsorbent loading = 0.025 g/L), room temperature, initial pH ~ 6.5 (before addition of the adsorbent), stirring rate: 600 rpm.

Table S4. Antibiotics adsorption kinetic parameters estimated on the basis of pseudo-first order (PFO) and pseudo-second order (PSO) models [*Clean. Eng. Technol.* 1 (2020) 100032, doi:10.1016/j.clet.2020.100032]. Representative graphs used for estimation of the reaction kinetics are shown in Fig. S28.[a]

Adsorbate	q_e (exp)[b] [mg/g]	PFO			PSO		
		k [1/min]	q_e (cal)[c] [mg/g]	R^2	k [g/mg/min]	q_e (cal)[c] [mg/g]	R^2
CIP	427.5	0.01700	226.8	0.92429	0.00026	436.7	0.99940
TC	413.2	0.02716	245.4	0.94531	0.00034	427.4	0.99969
AMX	228.9	0.03468	140.8	0.93917	0.00074	236.4	0.99940
SMX	188.1	0.03039	75.4	0.87696	0.00173	190.5	0.99990

[a] *Adsorption conditions*: 200 mL of the antibiotic solution (C_0 = 15 mg/L), 5 mg of sHCP1 (adsorbent loading = 0.025 g/L), initial pH ~ 6.5 (before addition of the adsorbent), room temperature, stirring rate: 600 rpm.

[b] Maximum adsorption capacity of the sample derived from the experiment.

[c] Maximum adsorption capacity of the sample calculated from the kinetic model.

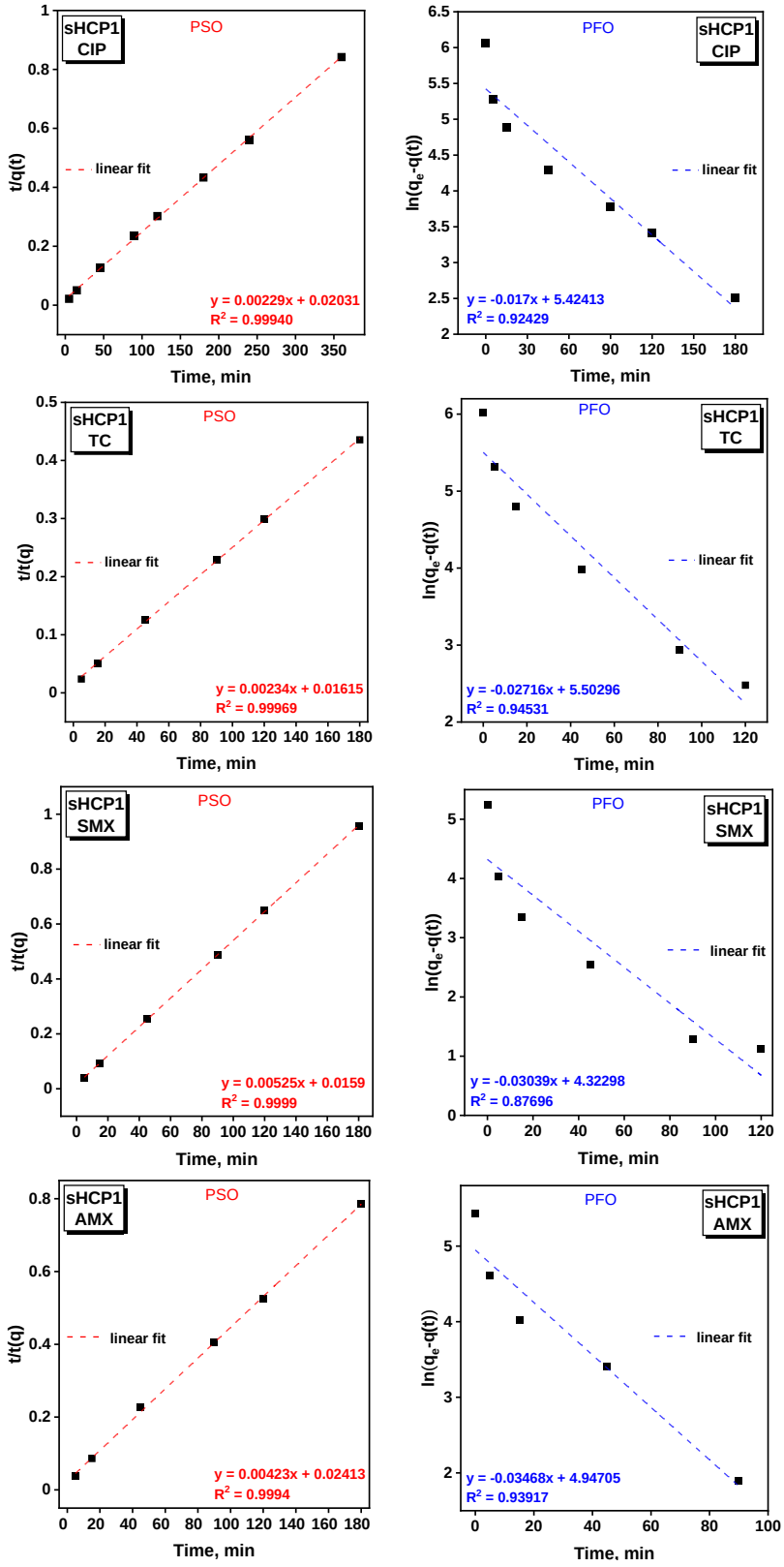

Fig. S28. Graphs used for assessing the antibiotics adsorption kinetics on the sHCP1 adsorbent. PFO and PSO stand for pseudo-first order and pseudo-second order kinetic model, respectively. *Adsorption conditions:* 200 mL of the antibiotic solution (C_0 = 15 mg/L), 5 mg of sHCP1 (adsorbent loading = 0.025 g/L), initial pH ~ 6.5 (before addition of the adsorbent), room temperature, stirring rate: 600 rpm.

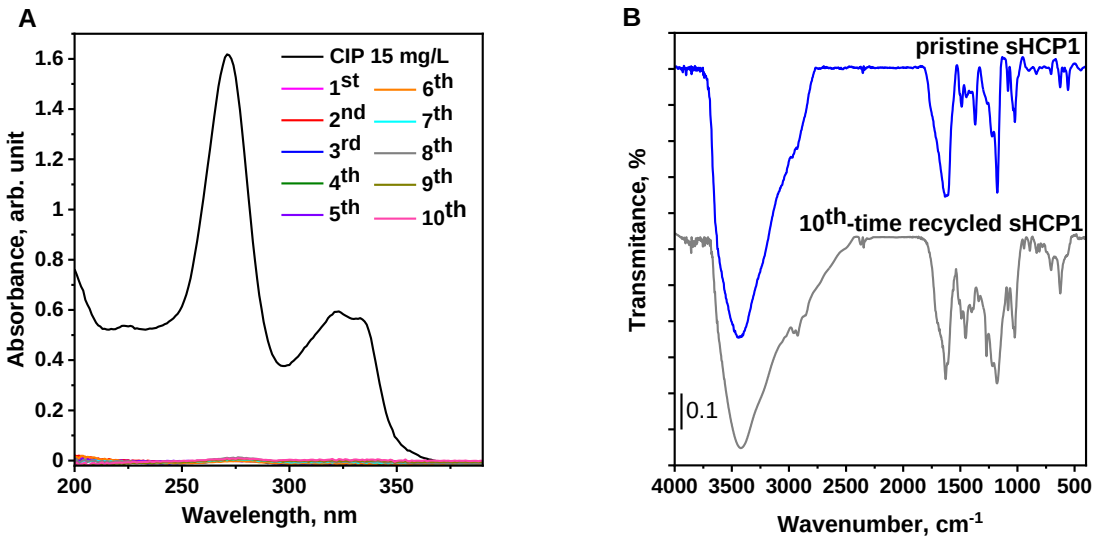

Fig. S29. (A) UV-vis absorption spectra of liquid phase recorded during removal of CIP in the presence of sHCP1 after different adsorption cycles. *Adsorption conditions*: 200 mL of the antibiotic solution (C_0 = 15 mg/L), 20 mg of the polymer (adsorbent loading = 0.100 g/L), initial pH ~ 6.5 (before addition of the adsorbent), room temperature, stirring rate: 600 rpm. (B) FTIR spectra of the pristine and 10th-time recycled sHCP1 polymer.

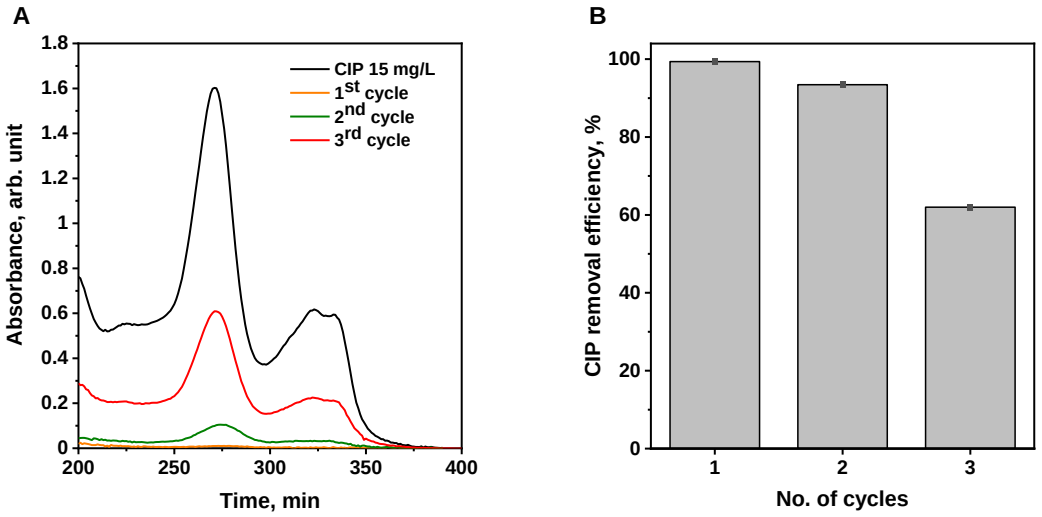

Fig. S30. (A) UV-vis absorption spectra of liquid phase recorded during removal of CIP in the presence of sHCP1 after different adsorption cycles using ethanol as regeneration agent. (B) Stability of sHCP1 polymer during 3 adsorption-desorption cycles using ethanol as regeneration agent. *Adsorption conditions*: 200 mL of ciprofloxacin solution (C_0 = 15 mg/L), 20 mg of adsorbent (adsorbent loading = 0.100 g/L), room temperature, initial pH ~ 6.5, stirring rate: 600 rpm.

Table S5. Adsorption capacity of selected materials dedicated to the adsorptive removal of CIP, TC, AMX and SMX.

Adsorbent	Type of adsorbent	Adsorbent loading [g/L]	C_o [mg/L]	pH	Temp. [°C]	Time [min]	Adsorption capacity (q_e) [mg/g]	References
Ciprofloxacin								
MgO/Chit/GO	Chitosan-based nanocomposite	0.5	30-1500	7.0	25	360	22.7	*Microchim. Acta.* 186 (2019) 459, doi:10.1007/s00604-019-3563-x.
CBHB	Chitosan-based hydrogel	0.25	50	3.0	30	-	36.7	*Sci. Total Environ.* 639 (2018) 560, doi:10.1016/j.scitotenv.2018.05.129.
JLUE-HCOPs	Covalent organic polymer	1.0	20	6.0	RT	2880	84.0	*Eur. Polym. J.* 123 (2020) 109445. doi:10.1016/j.eurpolymj.2019.109445
CPS	Agriculture waste coated with zinc oxide	200.0-10000.0	30-70	3.0-9.0	25-35	0-120	92.4	*Arab. J. Chem.* 13 (2020) 4629, doi:10.1016/j.arabjc.2019.10.010.
GH	Porous graphene hydrogel	-	50	6.0	25	-	235.6	*Sci. Rep.* 5 (2015) 1, doi: 10.1038/srep13578.
sHCP1	Hyper-cross-linked polymer	0.025	15	6.5	RT	180	427.5	This work
MB_{CP}	Modified bentonite	0.2	100	6.0	25	0-90	457.0	*Sep. Purif. Technol.* 274 (2021) 119059, doi:10.1016/j.seppur.2021.119059.
Tetracycline								
CPS	Agriculture waste coated with zinc oxide	200.0-10000.0	30-70	3.0-9.0	25-35	0-120	98.7	*Arab. J. Chem.* 13 (2020) 4629, doi:10.1016/j.arabjc.2019.10.010.
NaY zeolite	Zeolite	500.0	80	7.0	30	1440	201.8	*J. Clean. Prod.* 172 (2018) 602, doi:10.1016/j.jclepro.2017.10.180.
SKTPS	Hyper-cross-linked polymer	1.0	0.044	7.0	RT	5	209.0	*ACS Appl. Mater. Interfaces.* 14 (2022) 7369, doi:10.1021/acsami.1c24393.

HCP-BPA-Na	Hyper-cross-linked polymer	0.075	0.125	3.0	25-45	-	268.1	*J. Water Process Eng.* 40 (2021) 101902, doi:10.1016/j.jwpe.2020.101902.
HCP-MAH	Hyper-cross-linked polymer	0.125	30	7.0	25	1440	273.2	*J. Environ. Chem. Eng.* 9 (2021) 106047, doi:10.1016/j.jece.2021.106047.
La-impregnated MCM-41	Zeolite	0.06	100	7.0	RT	1440	303.3	*Environ. Technol.* 31 (2010) 233, doi:10.1080/09593330903453210.
ZIF-8	Metal-organic framework	0.5	50	4.0	30	240	312.5	*J. Hazard. Mater.* 366 (2019) 563, doi:10.1016/j.jhazmat.2018.12.047.
sHCP1	Hyper-cross-linked polymer	0.025	15	6.5	RT	180	413.2	This work
HCP-COOH	Hyper-cross-linked polymer	0.125	30	7.0	25	1440	418.4	*J. Environ. Chem. Eng.* 9 (2021) 106047, doi:10.1016/j.jece.2021.106047.
MB_{CP}	Modified bentonite	0.2	100	6.0	25	0-90	476.0	*Sep. Purif. Technol.* 274 (2021) 119059, doi:10.1016/j.seppur.2021.119059.
Amoxicillin								
CPS	Agriculture waste coated with zinc oxide	200.0-10000.0	30-70	3.0-9.0	25-35	0-120	132.2	*Arab. J. Chem.* 13 (2020) 4629, doi:10.1016/j.arabjc.2019.10.010.
PIM-1	Polymer of intrinsic microporosity	0.4	73	7.0	RT	1440	208.6	*Sci. Rep.* 10 (2020) 1, doi:10.1038/s41598-020-57616-4.
MMT K10	Montmorillonite K10	0.1	50	7.5	30	120	215.1	*Colloids Surf., A Physicochem. Eng. Asp.* 611 (2021) 125792, doi:10.1016/j.colsurfa.2020.125792.
sHCP1	Hyper-cross-linked polymer	0.025	15	6.5	RT	180	228.9	This work
MIL-53(Al)	Metal-organic framework	0.1	50	7.5	30	120	258.4	*J. Chem. Eng. Data* 66 (2021) 389, doi:10.1021/acs.jced.0c00736.
Sulfamethoxazole								

HA	Humus component	4.0	100	-	25	2880	7.5	*RSC Adv.* 7 (2017) 50449, doi:10.1039/c7ra06231a.
sHCP1	Hyper-cross-linked polymer	0.025	15	6.5	RT	180	188.1	This work
GO	Graphite oxide	-	40	5.0	-	2880	240.0	*J. Hazard. Mater.* 282 (2015) 201, doi:10.1016/j.jhazmat.2014.03.063.
HPOP-3	Porous organic polymer	0.05	20	4.5	25	180	331.9	*Environ. Sci. Nano.* 9 (2022) 730, doi:10.1039/d1en01031j.